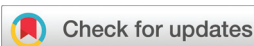


RESEARCH ARTICLE

[View Article Online](#)
[View Journal](#) | [View Issue](#)



Cite this: *Org. Chem. Front.*, 2025, **12**, 5525

Received 7th May 2025,
Accepted 10th June 2025
DOI: 10.1039/d5qo00725a
rsc.li/frontiers-organic

Kinetic resolution of trifluoromethylated heterobenzhydrols via hydrogen-acceptor-free Ir-catalyzed heteroaryl-selective C–H silylation†

Ryu Tadano, Takeshi Yasui and Yoshihiko Yamamoto *

Kinetic resolution of benzhydrols via intramolecular C–H silylation is an efficient method for the preparation of chiral benzhydrols. However, the previously reported methods required sterically demanding phenyl rings to achieve group-selective C–H silylation. Herein, we report the kinetic resolution of trifluoromethylated heterobenzhydrols, bearing both phenyl and thiophene rings, via heteroaryl-selective C–H silylation. We conducted computational studies on the factors influencing the enantioselectivity and heteroaryl selectivity.

Introduction

Fluorine-containing compounds have significant applications in pharmaceuticals¹ and agrochemicals.² In particular, the CF₃ group is the most common polyfluoroalkyl substituent in newly approved drugs.³ However, most trifluoromethylated pharmaceuticals are benzotrifluoride derivatives. Although numerous chiral pharmaceuticals with the CF₃ group on an sp² carbon atom are commercially available, only a few drugs, namely efavirenz, telotristat ethyl, and suzetrigine, have the CF₃ group at the stereogenic carbon center (Fig. 1A).¹ Given the numerous reports on racemic bioactive compounds with the CF₃ group on a sp³ carbon center chiral trifluoromethylated compounds have high potential value as pharmaceuticals. Notably, trifluoromethylated aryl heteroaryl carbinols (heterobenzhydrols) are significant because they are found in bioactive compounds such as selective androgen receptor modulators (SARMs) and liver X receptor (LXR) agonists (Fig. 1A),⁴ leading to increasing demand for their enantioselective synthesis.

Chiral trifluoromethylated benzhydrols are usually synthesized via enantioselective nucleophilic addition reactions.⁵ However, this method has several limitations. First, organometallic nucleophiles are unstable and have low functional group tolerance. Second, enantioselective nucleophilic addition often requires stoichiometric amounts of chiral ligands. Therefore, we focused on enantioselective desymmetrization via

C–H silylation as a novel synthetic approach. Hartwig, Shi, and their coworkers developed enantioselective desymmetrization of benzhydrols using Rh- or Ir-catalyzed intramolecular C–H silylation: however, they did not investigate tertiary alcohol substrates.⁶ Inspired by their research, we developed enantioselective desymmetrization of trifluoromethylated tertiary benzhydrols, which is the first example of the synthesis of trifluoromethylated benzhydrols via enantioselective desymmetrization (Fig. 1B).⁷ Notably, no hydrogen acceptor was required for our method, in contrast to the use of norbornene as the hydrogen acceptor that was essential in previous methods. A general limitation of enantioselective desymmetrization is that unsymmetrical benzhydrol substrates with different aryl groups cannot be used. In addition, heterobenzhydrols have not yet been used as substrates for enantioselective desymmetrizations. Another approach for the synthesis of chiral trifluoromethylated benzhydrols is the kinetic resolution of unsymmetrical benzhydrols bearing different aryl groups. Kinetic resolution requires a group-selective reaction involving one of the two aryl groups. Hartwig, Shi, and their coworkers achieved kinetic resolution of unsymmetrical secondary benzhydrols via C–H silylation by introducing a substituent at the *ortho* position of one phenyl ring to reduce its reactivity by steric repulsion.^{6b} Similarly, we succeeded in the kinetic resolution of unsymmetrical tertiary trifluoromethylated benzhydrols bearing a sterically demanding phenyl rings substituted at the 2- or 3,5-positions (Fig. 1C).⁷ However, group selectivity driven by steric repulsion imposes significant constraints on substrate design owing to the requirement for sterically demanding phenyl groups.

Therefore, we focused on the kinetic resolution of heterobenzhydrols. Previous attempts to achieve enantioselective desymmetrization of bis(1-methyl-3-indolyl)carbinol were unsuccessful. The inferior reactivity of the indole ring in our

Department of Basic Medicinal Sciences, Graduate School of Pharmaceutical Sciences, Nagoya University, Chikusa, Nagoya 464-8601, Japan.

E-mail: yamamoto.yoshihiko.y9@mail.nagoya-u.ac.jp

† Electronic supplementary information (ESI) available: Experimental and computational details, compound characterization data, ¹H and ¹³C NMR charts. See DOI: <https://doi.org/10.1039/d5qo00725a>



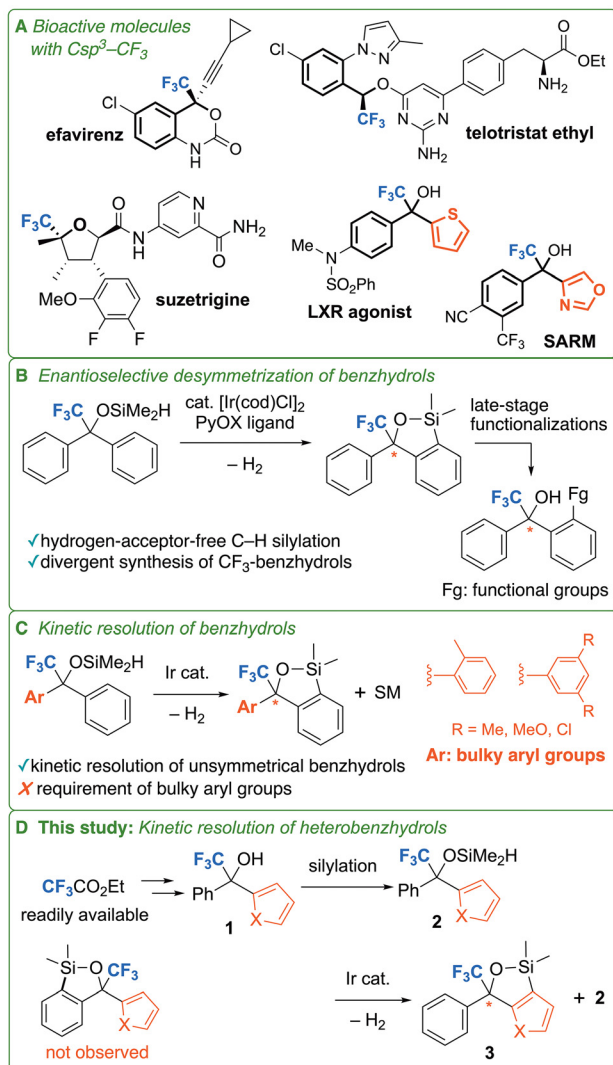


Fig. 1 Background of this study. (A) Bioactive molecules bearing the CF_3 group on an sp^3 carbon. (B) Enantioselective desymmetrization of trifluoromethylated benzhydrols. (C) Kinetic resolution of trifluoromethylated benzhydrols. (D) Kinetic resolution of trifluoromethylated heterobenzhydrols.

method suggests that unsymmetrical benzhydrols bearing both phenyl and inactive heteroaryl groups enable group-selective reactions without the introduction of the sterically demanding phenyl group. In this study, we investigated the kinetic resolution of heterobenzhydrols bearing phenyl groups and five-membered heteroaromatic rings (Fig. 1D). Contrary to our expectations, the heteroaromatic rings underwent C–H silylation preferentially over the phenyl groups.

Results and discussion

Reaction development

Among the representative five-membered heteroaromatic compounds, thiophene was selected because of its “chemical proximity” to benzene.⁸ Trifluoromethylated phenyl thiienyl carbinol **1a** was prepared *via* the reaction of trifluoroacetophenone derived from ethyl trifluoroacetate with thienyllithium and subsequent silylation of the hydroxy group with chlorodimethylsilane afforded hydrosilane **2a** (see ESI†). The prepared **2a** was subjected to C–H silylation under conditions optimized in our previous study; however, to our surprise, thienoxasilole **3a** was exclusively obtained instead of the expected benzoxasilole **3a'** (Fig. 2A).^{9,10} The reaction of the previously employed benzhydrol silyl ethers took 5 h to complete,⁷ whereas **2a** reacted completely within 2 h. This fact suggests that thiophene has a higher reactivity than benzene toward C–H silylation. When the dimethylsilyl group was replaced by a diethylsilyl group, we observed a significantly lower reaction rate even at a higher temperature (80 °C), and partial desilylation was also detected (Fig. S1, ESI†). Based on these results, we shifted our focus toward developing a heteroaryl-selective C–H silylation. We investigated the kinetic resolution of **2a** by stopping the reaction at approximately half conversion (Fig. 2B). However, partial desilylation of **2a** to **1a** occurred during purification by silica gel column chromatography, and the separation of **1a** from **3a** was difficult. We envisaged that modifying the dimethylsilyl group of unreacted **2a** to a triallylsilyl group would enhance kinetic stability. Therefore, we confirmed that the Ir-catalyzed hydrosilylation of **2a** with 4-vinylanisole

and the kinetic resolution of **2a** were successful (Fig. 2C).

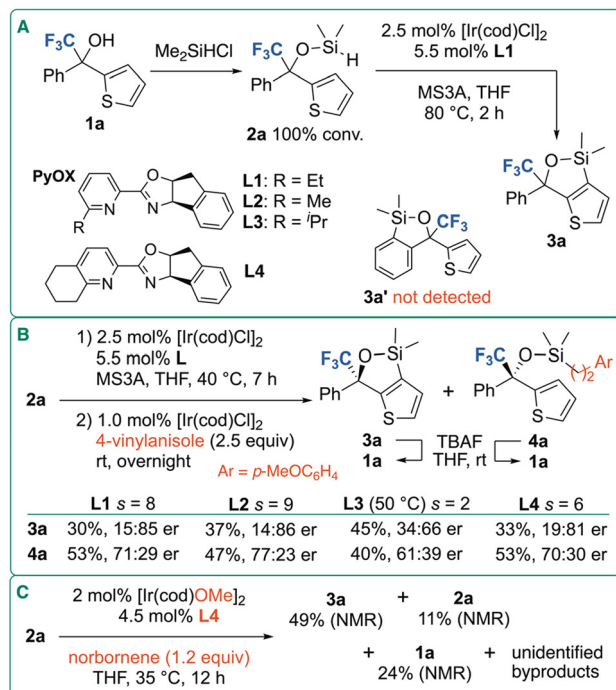


Fig. 2 Reaction development. (A) Ir-catalyzed intramolecular dehydrogenative silylation of **2a** at full conversion. (B) Kinetic resolution of **2a**. Enantiomeric ratio (er) was determined by chiral HPLC after desilylation of the products. Selectivity values (s) were determined according to $s = \ln[1 - c(1 + ee_p)] / \ln[1 - c(1 - ee_p)]$ (c : conversion based on product yields, ee_p : product enantiomeric excess). (C) Reaction of **2a** under conditions previously reported (ref. 6b).



afforded **4a**, completely suppressing its desilylation (Table S1, ESI†).¹¹ Next, we investigated the effect of chiral ligands on the enantioselectivity. Because **3a** and **4a** were unsuitable for chiral HPLC analysis, we evaluated their enantiopurity after desilylation. Previous studies showed that chiral pyridine-oxazoline (PyOX) ligands that contain indane-fused oxazoline and 6-substituted pyridine rings achieved high enantioselectivity in C–H silylation.^{6b,7} Therefore, we used the chiral ligands **L1–L4** for the kinetic resolution of **2a**. PyOX ligands **L1** and **L2**, bearing the ethyl and methyl groups, respectively, on the pyridine ring, afforded nearly identical results, with **L2** showing slightly higher enantioselectivity. The use of the previously reported ligand (**L4**)^{6b} led to slight decrease in enantioselectivity. Generally, **3a** was obtained with higher enantiopurity than **4a**, independent of the conversion of **2a**. In contrast, **L3**, which bears a bulkier isopropyl group, showed a marked

decrease in enantioselectivity. Therefore, **L2** was selected as the optimal ligand. We also applied the kinetic resolution conditions developed by Hartwig and Shi to **2a** (Fig. 2C).^{6b} In the presence of norbornene as the H₂ acceptor, **2a** was treated with 2 mol% $[\text{Ir}(\text{cod})\text{OMe}]_2$ and 4.5 mol% PyOX ligand **L4** at 35 °C for 12 h, affording **3a** in 49% yield (¹⁹F NMR), albeit with several unidentified byproducts being observed; however, substantial amounts of **1a** was formed by desilylation of **2a**, hampering the separation of **3a**. Therefore, we used our acceptorless conditions for further investigations.

Next, we investigated the substrate scope under optimal conditions (Fig. 3). Hydrosilanes **2b–i** with substituents on the phenyl ring underwent thiophene-selective C–H silylation, affording **3b–3i** with 19 : 81–10 : 90 er. However, *o*-tolyl-substituted **3d** decomposed during isolation. We assumed that the decomposition of **3d** was due to the strain caused by the

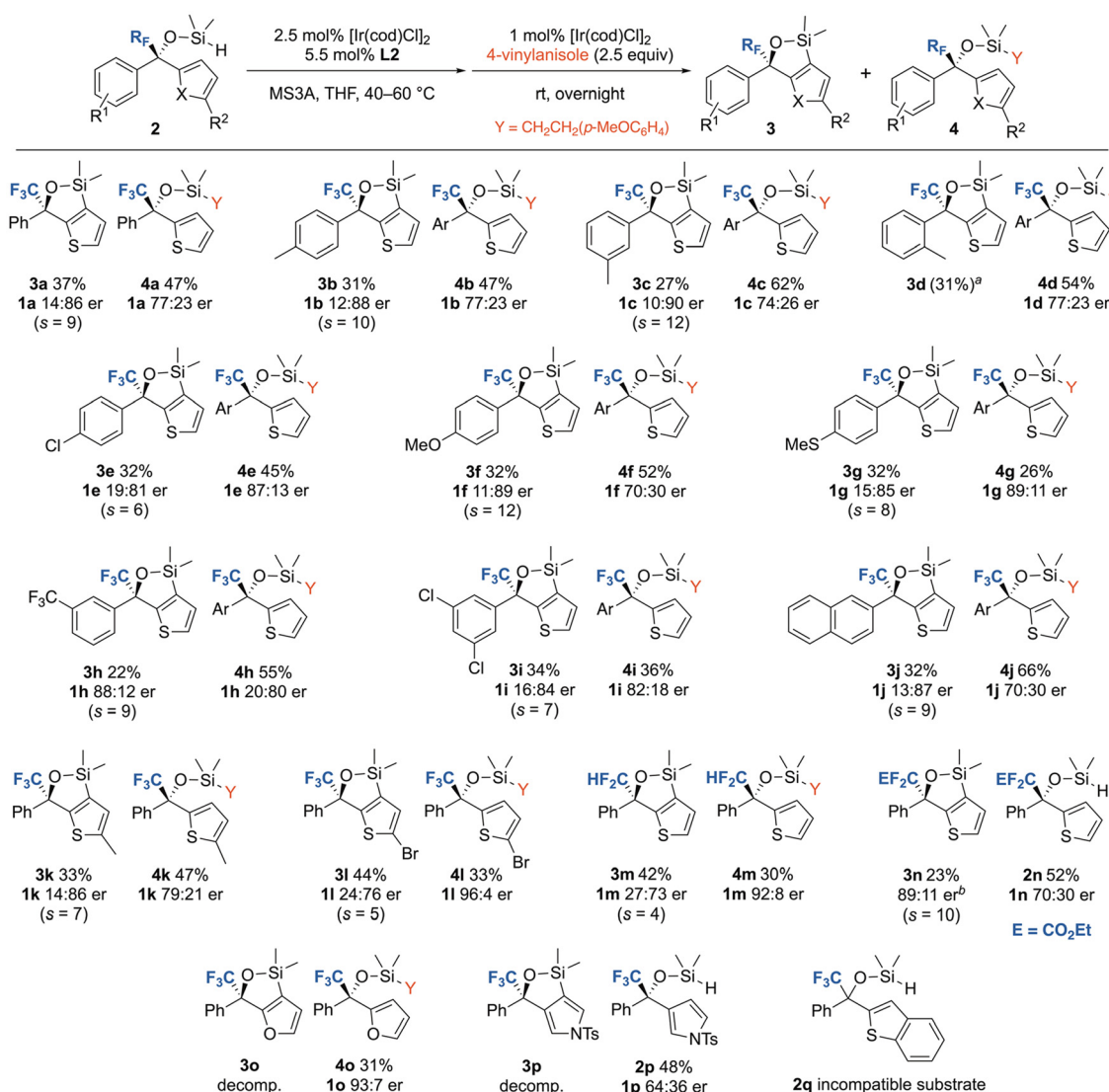


Fig. 3 Scope of trifluoromethylated heterobenzhydrol substrates. The er values were determined after desilylation using chiral HPLC. The absolute configurations were assigned by analogy (for details, see ESI†).^a Yield determined by ¹⁹F NMR. ^b The er value was determined without desilylation using chiral HPLC.



2-methyl substituent. Both electron-donating (OMe and SMe) and -withdrawing (Cl and CF₃) groups were compatible. The reaction of **2j** with a 2-naphthyl group afforded **3j** in 32% yield with 13 : 87 er. Similarly, 5-methylthienyl-substituted **2k** and 5-bromothienyl-substituted **2l** afforded **3k** and **3l**, albeit with a slight erosion of er for the latter. Substrates **2m** and **2n**, bearing CF₂H and CF₂CO₂Et groups at the benzylic position, respectively, underwent thiophene-selective silylation to afford **3m** and **3n**; however, the er of **3m** was lower, indicating that the smaller CF₂H group decreases enantioselectivity. Notably, both **3n** and unreacted **2n**, bearing bulky CF₂CO₂Et groups, were isolated using column chromatography with diol silica gel, eliminating the need for the hydrosilylation of **2n**. The C–H silylation of **2o**, which bears a furan ring, proceeded smoothly. However, furooxasilole **3o** was unstable and decomposed rapidly upon exposure to air (for details, see ESI†). Therefore, the enantioselectivity was analyzed for **4o**, which exhibited a high er of 93 : 7. The reaction of **2p** bearing a *N*-tosylated 2-pyrrolyl ring also proceeded with a similar heterocycle selectivity. Although **3p** was very unstable to afford a complex product mixture after purification, unreacted **2p** was recovered without its hydrosilylation. The enantioselectivity of **2p** was analyzed after desilylation, which exhibited a much lower er of 64 : 36. In contrast, the reaction of benzothienyl-

substituted **2q** was significantly slow at 40 °C, and the reaction at elevated temperatures yielded complex product mixtures.

To explore whether the aryl group, which does not participate in the reaction, can be replaced with alkyl groups, *n*-butyl-substituted **2r** was subjected to C–H silylation (Fig. 4A). However, **3r** was obtained with low er (44 : 56). Because it was hypothesized that the high flexibility of the *n*-butyl group of **2r** led to the decrease in er, heterobenzhydrol derivative **2s**, bearing a more constrained *c*-hexyl group, was examined; however, **3s** was obtained with a similarly low er. Moreover, heterobenzhydrol **2t** and **2u** bearing an ethyl or methyl group instead of the CF₃ group was investigated to examine the role of the CF₃ group (Fig. 4B). The reaction of **2t** with the ethyl group, which has a comparable van der Waals volume with the CF₃ group,¹² under standard reaction conditions produced the corresponding products **3t** and **4t**. Although **4t** was isolated in 21% yield, thienooxasilole **3t** is unstable and decomposed during silica gel chromatography. The enantiomeric ratio of **4t** was evaluated after desilylation as 86 : 14. Similarly, the reaction of **2u** with the smaller methyl group afforded **4u** in 20% yield, and its enantiomeric ratio evaluated after desilylation was lower (64 : 36) than that of **4t**. Therefore, the CF₃ group is beneficial for the stability of thienooxasilole products as well as enantioselectivity; however, it is not essential for the Ir-catalyzed heteroaryl-selective dehydrogenative silylation. This

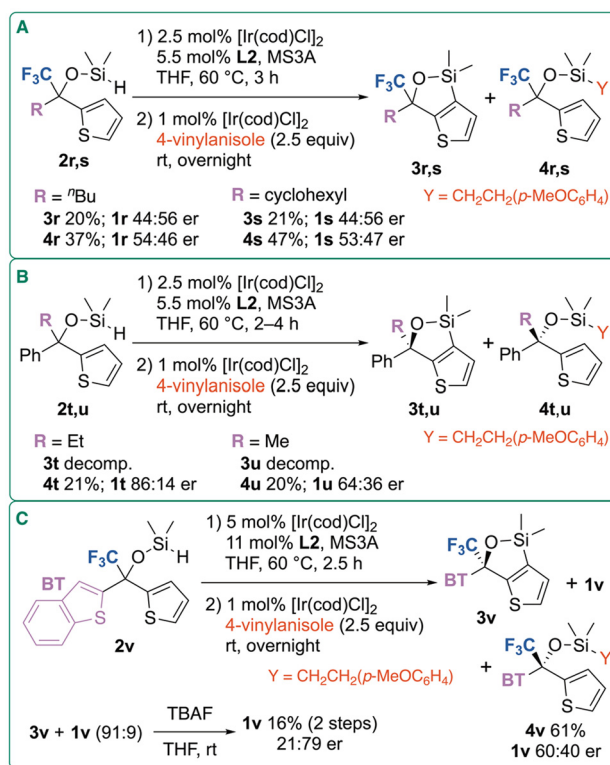


Fig. 4 Kinetic resolution of other substrates. The yields refer to isolated products, and the er values were determined after desilylation using chiral HPLC. (A) Kinetic resolution of trifluoromethylated thienyl carbinols. (B) Kinetic resolution of heterobenzhydrols without a CF₃ group. (C) Kinetic resolution of a bisheteroarylmethanol.

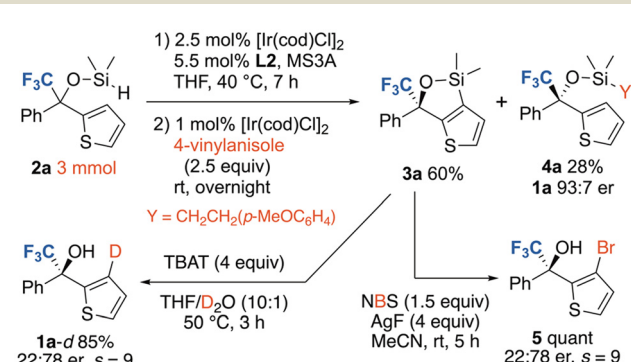


Fig. 5 Scale-up synthesis of **3a** and its transformations.

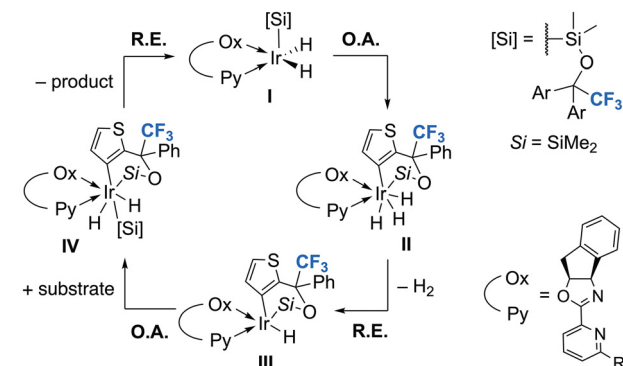


Fig. 6 Proposed catalytic cycle.



result is in striking contrast to our previous observation that the CF_3 group is necessary for efficient reactions in the enantioselective desymmetrization of benzhydrols.⁷

Because the benzothienyl group in **2q** did not undergo C–H silylation (Fig. 3), the kinetic resolution of silane **2v**, bearing both thiienyl and benzothienyl groups, was subjected to the standard Ir-catalyzed C–H silylation conditions. Although the C–H bond on the thiienyl group was selectively activated, the reaction was sluggish and partial desilylation of **2v** occurred during the prolonged reaction. Therefore, the reaction of **2v** was conducted with an increased catalyst loading for 2.5 h (Fig. 4c). Because the separation of thienooxasilole **3v** from **1v** was impossible, the treatment of an inseparable mixture (**3v/1v** 91 : 9) with TBAF afforded **1v** with 21 : 79 er, albeit in a low yield (16%). In contrast, **4v** was isolated in 61% yield and its enantioselective ratio was determined as 60 : 40, after desilylation.

The kinetic resolution of **2a** was performed at a 3 mmol scale to obtain **3a** in 60% yield, which was further transformed into deuterated heterobenzhydrol **1a-d** in 85% yield with 22 : 78 er (Fig. 5). Upon treatment of **3a** with NBS in the presence of AgF , brominated heterobenzhydrol **5** was also quantitatively obtained with 22 : 78 er.

Computational mechanistic study

In our previous study, we proposed a reaction mechanism for the C–H silylation of trifluoromethylated benzhydrols without a hydrogen acceptor.⁷ A similar mechanism is expected for heterobenzhydrols; however, C–H activation occurs preferably on the thiophene ring rather than the phenyl ring (Fig. 6). Initially, the *in situ*-generated Ir(III) dihydride species **I**¹³ undergoes the thiienyl–H oxidative addition, leading to Ir(V) trihydride species **II**.¹⁴ This is the rate- and enantio-determining

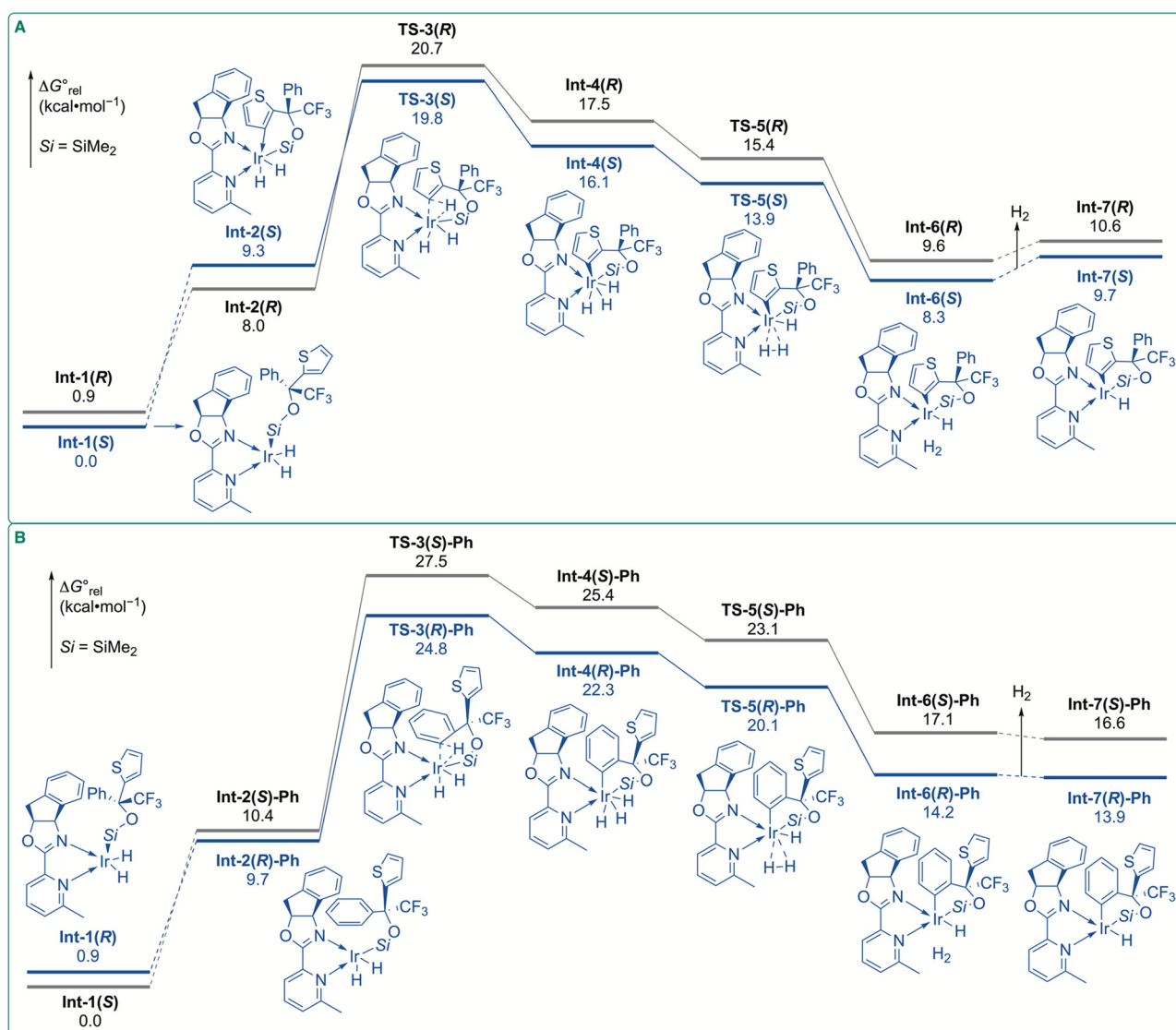


Fig. 7 Gibbs energy profiles: [SMD:THF] M06/SDD-6-311+G(d,p)//B3LYP-D3(BJ)/LanL2DZ-6-31G(d) at 298.15 K and 1 atm. (A) Profiles of thienyl–H activation. (B) Profile of Ph–H activation. Structures of stationary points and transition states for the major pathways are shown.



step. The subsequent reductive elimination of H_2 generates Ir(III) monohydride species **III**.^{14,15} The H_2 generation in the catalytic reaction was monitored by ^1H NMR spectroscopy in our previous study.⁷ Although the C–H oxidative addition and subsequent reductive elimination of H_2 are endergonic and reversible, facile extrusion of H_2 gas from the reaction solutions renders the overall reaction irreversible.¹⁶ Finally, the Si–H oxidative addition of another substrate is followed by the reductive elimination of thienooxasilole from resulting **IV** to restore **I**.

To gain insights into the enantio-determining step, we performed density functional theory (DFT) calculations at the SMD (THF) M06/SDD-6-311+G(d,p)//B3LYP-D3(BJ)/LanL2DZ-6-31G(d) level of theory (for details, see ESI†) on the C–H oxidative addition and subsequent reductive elimination of H_2 (Fig. 7A). Ir(III) active species **I** has a square pyramidal geometry with a silyl ligand at the apical position (Fig. 6).^{13,17} We assumed that C–H silylation occurs from the same face with the indane moiety of the ligand because the π – π interactions between the indane moiety and thiophene ring stabilize the transition state for the C–H activation steps (*vide infra*). In fact, C–H silylation from the opposite face with the indane moiety was found to be less efficient (Fig. S2, ESI†). Ir(III) species with the silyl group at the apical position were located as **Int-1(S)** and **Int-1(R)**, and **Int-1(R)** is less stable than **Int-1(S)** by 0.9 kcal mol⁻¹. To provide an empty coordination site for C–H oxidative addition, the geometric isomerization of **Int-1(S)** and **Int-1(R)** leads to **Int-2(S)** and **Int-2(R)**, in which the silyl ligand is located at the basal position. **Int-2** is approximately 8 kcal mol⁻¹ less stable than **Int-1** owing to the strong *trans* influence of the silyl group.¹⁸ The transition states for the C–H oxidative addition of the thiophene ring were identified as **TS-3(S)** and **TS-3(R)**, with the activation barriers of 10.5 and 12.7 kcal mol⁻¹ from precursor complex **Int-2(S)** and **Int-2(R)**, respectively. The subsequent reductive elimination of H_2 is almost barrierless (Fig. S3, ESI†).

Because the oxidative addition of the silane substrate is facile and reversible,^{6b} **Int-1(S)** and **Int-1(R)** are in equilibrium through Ir(V) trihydride species (Fig. S4, ESI†). Because the activation barriers are less than 17 kcal mol⁻¹, this interconversion is more facile than the subsequent thiophene C–H activation. The energetic span between **Int-1(S)** and **TS-3(S)** (19.8 kcal mol⁻¹) is lower than that between **Int-1(S)** and **TS-3(R)** (20.7 kcal mol⁻¹). Consequently, the (S)-enantiomer was predicted to be formed preferentially, which was in good agreement with the absolute configuration of the experimentally obtained products. The centroid–centroid distance between the indane and thiophene rings in **TS-3(S)** is shorter than that in **TS-3(R)** (Fig. 8A). Therefore, the π – π interactions between the indane and thiophene rings are expected to be stronger in **TS-3(S)** than in **TS-3(R)**. Non-covalent interaction (NCI) analysis¹⁹ confirmed that the π – π interactions are more favorable in **TS-3(S)** (Fig. S5, ESI†).

Calculations were also performed for the C–H activation of the phenyl ring to compare the reactivity of thiophene and benzene (Fig. 7B). The transition states for Ph–H oxidative

addition were identified as **TS-3(S)-Ph** and **TS-3(R)-Ph**, with activation barriers of 17.1 and 15.1 kcal mol⁻¹ from precursor complexes **Int-2(S)-Ph** and **Int-2(R)-Ph**, respectively. The energetic differences between **Int-1(S)** and **TS-3(S)-Ph** (27.5 kcal mol⁻¹) and between **Int-1(S)** and **TS-3(R)-Ph** (24.8 kcal mol⁻¹) are higher than those for **TS-3(S)** and **TS-3(R)**. Thus, C–H activation on the thiophene ring is predicted to be favored compared to that on the phenyl ring, consistent with the experimental results.

Our previous DFT study of the C–H silylation of benzhydrol-derived hydrosilane suggested that the final reductive elimination of the benzoxasilole product occurred *via* the oxidative addition of the hydrosilane substrate.⁷ A similar pathway was also found for the reductive elimination of the thienooxasilole product; the oxidative addition of the hydrosilane substrate to **Int-7(S)** generates Ir(V) metallacyclic intermediate **Int-9(S,R)** or **Int-9(S,S)**, which undergoes the facile reductive elimination of thienooxasilole with the regeneration of the active catalyst (Fig. S6, ESI†). These results support the proposed Ir(III)/Ir(V) catalytic cycle as outlined in Fig. 6. The reductive elimination of the thienooxasilole product from **Int-9(R,R)** or **Int-9(R,S)** also proceeds similarly; however, it is less efficient than that from **Int-9(S,R)/Int-9(S,S)** as the energetic span between **Int-7** and **TS-10** is higher for (R)-isomers than for (S)-isomers.

To understand why the activation barrier for the C–H oxidative addition of thiophene is lower than that of benzene, we investigated iridacycle intermediates **Int-4** formed from C–H oxidative addition. The relative Gibbs energy (ΔG_{rel}) of thie-

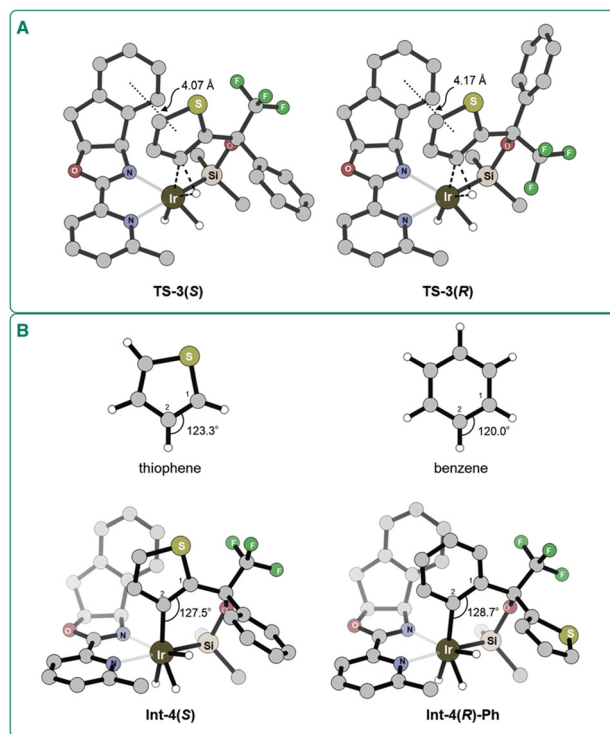


Fig. 8 Optimized geometries. (A) **TS-3(S)** and **TS-3(R)**. (B) Thiophene, benzene, **Int-4(S)**, and **Int-4(R)-Ph**.



noiridacycle **Int-4(S)** is 16.1 kcal mol⁻¹, whereas the $\Delta G_{\text{rel}}^{\circ}$ of benzoiridacycle **Int-4(R)-Ph** is 22.3 kcal mol⁻¹, indicating that benzoiridacycle **Int-4(R)-Ph** is less stable by 6 kcal mol⁻¹ than **Int-4(S)**. The C(1)–C(2)–H angle of thiophene is 123.3°, while the corresponding C(1)–C(2)–Ir angle in **Int-4(S)** is 127.5°, leading to a bond-angle strain of 4.2° (Fig. 8B). In contrast, the C(1)–C(2)–H angle of benzene is 120.0°, while the corresponding C(1)–C(2)–Ir angle in **Int-4(R)-Ph** is 128.7°, causing a bond-angle strain of 8.7°. Owing to the smaller ring strain of the thienoiridacycle than that of benzoiridacycle, the activation barrier of thienyl–H oxidative addition is reduced.²⁰

Conclusions

We achieved kinetic resolution of unsymmetrical trifluoromethylated heterobenzhydrols *via* Ir-catalyzed dehydrogenative C–H silylation. This approach is particularly useful for the synthesis of both enantiomers of heterobenzhydrols bearing the CF₃ and thienyl groups at the stereogenic center. DFT calculations revealed that the π – π interactions between the thiophene ring and ligand indenyl moiety play a crucial role in determining the enantioselectivity. Additionally, the smaller ring strain of the six-membered thienoiridacycle intermediate compared to that of the benzoiridacycle intermediate is the cause of the heteroaryl-selective C–H silylation.

Author contributions

Y. Y. conceived the project and wrote the manuscript. R. T. carried out the experimental and computational works, analyzed the experimental results, and wrote the manuscript. T. Y. discussed the results.

Conflicts of interest

There are no conflicts to declare.

Data availability

The data supporting this article have been included as part of the ESI.†

Acknowledgements

This research is partially supported by the Platform Project for Supporting Drug Discovery and Life Science Research (Basis for Supporting Innovative Drug Discovery and Life Science Research (BINDS) from AMED under Grant Number JP25ama121044) and JSPS KAKENHI (Grant Number JP22K05110). Computations were performed using the Research Center for Computational Science, Okazaki, Japan (Project: 24-IMS-C119 and 25-IMS-C120). R. T. acknowledges

the Inter-disciplinary Frontier Next-Generation Researcher Program of the Tokai Higher Education and Research System.

References

- (a) M. Inoue, Y. Sumii and N. Shibata, Contribution of Organofluorine Compounds to Pharmaceuticals, *ACS Omega*, 2020, **5**, 10633; (b) J. D. Osteen, S. Immani, T. L. Tapley, T. Indersmitten, N. W. Hurst, T. Healey, K. Aergeerts, P. A. Negulescu and S. M. Lechner, Pharmacology and Mechanism of Action of Suzetrigine, a Potent and Selective NaV1.8 Pain Signal Inhibitor for the Treatment of Moderate to Severe Pain, *Pain Ther.*, 2025, **14**, 655.
- Y. Ogawa, E. Tokunaga, O. Kobayashi, K. Hirai and N. Shibata, Current Contributions of Organofluorine Compounds to the Agrochemical Industry, *iScience*, 2020, **23**, 101467.
- M. Bassetto, S. Ferla and F. Pertusati, Polyfluorinated groups in medicinal chemistry, *Future Med. Chem.*, 2015, **7**, 527.
- Selected examples: (a) A. L. Handlon, L. T. Schaller, L. M. Leesnitzer, R. V. Merrihew, C. Poole, J. C. Ulrich, J. W. Wilson, R. Cadilla and P. Turnbull, Optimizing Ligand Efficiency of Selective Androgen Receptor Modulators (SARMs), *ACS Med. Chem. Lett.*, 2016, **7**, 83; (b) D. J. Kopecky, X. Y. Jiao, B. Fisher, S. McKendry, M. Labelle, D. E. Piper, P. Coward, A. K. Shiao, P. Escaron, J. Danao, A. Chai, J. Jaen and F. Kayser, Discovery of a New Binding Mode for a Series of Liver X Receptor Agonists, *Bioorg. Med. Chem. Lett.*, 2012, **22**, 2407; (c) X. Jiao, D. J. Kopecky, B. Fisher, D. E. Piper, M. Labelle, S. McKendry, M. Harrison, S. Jones, J. Jaen, A. K. Shiao, P. Escaron, J. Danao, A. Chai, P. Coward and F. Kayser, Discovery and Optimization of a Series of Liver X Receptor Antagonists, *Bioorg. Med. Chem. Lett.*, 2012, **22**, 5966.
- Selected reviews: (a) J.-A. Ma and D. Cahard, Asymmetric Fluorination, Trifluoromethylation, and Perfluoroalkylation Reactions, *Chem. Rev.*, 2004, **104**, 6119; J.-A. Ma and D. Cahard, Asymmetric Fluorination, Trifluoromethylation, and Perfluoroalkylation Reactions, *Chem. Rev.*, 2008, **108**, PR1; (b) Y.-Y. Huang, X. Yang, Z. Chen, F. Verpoort and N. Shibata, Catalytic Asymmetric Synthesis of Enantioenriched Heterocycles Bearing a C–CF₃ Stereogenic Center, *Chem. – Eur. J.*, 2015, **21**, 8664; (c) X.-H. He, Y.-L. Ji, C. Peng and B. Han, Organocatalytic Asymmetric Synthesis of Cyclic Compounds Bearing a Trifluoromethylated Stereogenic Center: Recent Developments, *Adv. Synth. Catal.*, 2019, **361**, 1923; (d) K. Hirano, Catalytic Asymmetric Construction of CF₃-Substituted Chiral sp³ Carbon Centers, *Synthesis*, 2022, 3708.
- (a) T. Lee, T. W. Wilson, R. Berg, P. Ryberg and J. F. Hartwig, Rhodium-Catalyzed Enantioselective Silylation of Arene C–H Bonds: Desymmetrization of Diarylmethanols, *J. Am. Chem. Soc.*, 2015, **137**, 6742;



(b) B. Su, T.-G. Zhou, X.-W. Li, X.-R. Shao, P.-L. Xu, W.-L. Wu, J. F. Hartwig and Z.-J. Shi, A Chiral Nitrogen Ligand for Enantioselective, Iridium-Catalyzed Silylation of Aromatic C–H Bonds, *Angew. Chem., Int. Ed.*, 2017, **56**, 1092; (c) B. Su and J. F. Hartwig, Development of Chiral Ligands for the Transition-Metal-Catalyzed Enantioselective Silylation and Borylation of C–H Bonds, *Angew. Chem., Int. Ed.*, 2022, **61**, e202113343.

7 Y. Yamamoto, R. Tadano and T. Yasui, Enantioselective Desymmetrization of Trifluoromethylated Tertiary Benzhydrols via Hydrogen-Acceptor-Free Ir-Catalyzed Fehydrogenative C–H Silylation: Decisive Role of the Trifluoromethyl Group, *JACS Au*, 2024, **4**, 807.

8 K. E. Horner and P. B. Karadakov, Chemical Bonding and Aromacity in Furan, Pyrrole, and Thiophene: A Magnetic Shielding Study, *J. Org. Chem.*, 2013, **78**, 8037.

9 (a) T. Ishiyama, K. Sato, Y. Nishio, T. Saiki and N. Miyaura, Regioselective Aromatic C–H Silylation of Five-membered Heteroarenes with Fluorodisilanes Catalyzed by Iridium(I) Complexes, *Chem. Commun.*, 2005, 5065; (b) H. Sun, Y. Cheng, H. Teng, X. Chen, X. Niu, H. Yang, Y.-M. Cui, L.-W. Xu and L. Yang, 3-Alkyl-2-pyridyl Directing Group-Enabled C2 Selective C–H Silylation of Indoles and Pyrroles via an Iridium Catalyst, *J. Org. Chem.*, 2022, **87**, 13346.

10 Single example of intramolecular C–H silylation of thiophene was reported: E. M. Simmons and J. F. Hartwig, Iridium-Catalyzed Arene *Ortho*-Silylation by Formal Hydroxyl-Directed C–H Activation, *J. Am. Chem. Soc.*, 2010, **132**, 17092.

11 S. P. Walsh, A. Lee and R. E. Maleczka, Jr, Iridium-Catalyzed Anti-Markovnikov Hydrosilylation of Vinylbenzenes with a Bis-Silane-Capped Double-Decker Silsesquioxane, *Organometallics*, 2024, **43**, 1085.

12 N. A. Meanwell, Fluorine and Fluorinated Motifs in the Design and Application of Bioisosteres for Drug Design, *J. Med. Chem.*, 2018, **61**, 5822.

13 (a) J. F. Harrod, D. F. R. Gilson and R. Charles, Oxidative Addition of Silicon Hydrides to Hydridocarbonyltris(tri-phenylphosphine)iridium(I), *Can. J. Chem.*, 1969, **47**, 2205; (b) A. J. A. Chalk, A New Synthesis of Silyliridium Hydrides, *J. Chem. Soc. D*, 1969, 1207; (c) M. Zhang, J. Liang and G. Huang, Mechanism and Origins of Enantioselectivity of Iridium-Catalyzed Intramolecular Silylation of Unactivated C(sp³)-H Bonds, *J. Org. Chem.*, 2019, **84**, 2372.

14 M. A. Esteruelas, A. Martínez, M. Oliván and E. Oñate, Kinetic Analysis and Sequencing of Si–H and C–H Bond Activation Reactions: Direct Silylation of Arenes Catalyzed by an Iridium-Polyhydrides, *J. Am. Chem. Soc.*, 2020, **142**, 19119.

15 (a) P. P. Deutsch and R. Eisenberg, Synthesis and Reactivity of Propionyliridium Complexes. Competitive Reductive Elimination of C–H and H–H Bonds from a Propionylidihydridoiodiridium Complex, *J. Am. Chem. Soc.*, 1990, **112**, 714; (b) P. P. Deutsch and R. Eisenberg, Synthesis and Reactivity of Ethyliridium Complexes. Reductive Elimination of C–H and H–H Bonds from an Ethyldihydridoiodiridium Complex, *Organometallics*, 1990, **9**, 709.

16 T. Ishiyama, T. Saiki, E. Kishida, I. Sasaki, H. Ito and N. Miyaura, Aromatic C–H Silylation of Arenes with 1-Hydrosilatrane Catalyzed by an Iridium(I)/2,9-dimethyl-phenanthroline (dmphen) Complex, *Org. Biomol. Chem.*, 2013, **11**, 8162.

17 C. Karmel and J. F. Hartwig, Mechanism of the Iridium-Catalyzed Silylation of Aromatic C–H Bonds, *J. Am. Chem. Soc.*, 2020, **142**, 10494.

18 T. G. Appleton, H. C. Clark and L. E. Manzer, The trans-Influence: Its Measurement and Significance, *Coord. Chem. Rev.*, 1973, **10**, 335.

19 E. R. Johnson, S. Keinan, P. Mori-Sánchez, J. Contreras-García, A. J. Cohen and W. Yang, Revealing Noncovalent Interactions, *J. Am. Chem. Soc.*, 2010, **132**, 6498.

20 W. Guo, T. Zhou and Y. Xia, Mechanistic Understanding of the Aryl-Dependent Ring Formations in Rh(III)-Catalyzed C–H Activation/Cycloaddition of Benzamides and Methylenecyclopropanes by DFT Calculations, *Organometallics*, 2015, **34**, 3012.

